Multi-vessel cooperative speed regulation for ship manipulation in towing scenarios

Du, Zhe; Negenborn, Rudy R.; Reppa, Vasso

DOI
10.1016/j.ifacol.2021.10.120

Publication date
2021

Document Version
Final published version

Published in
IFAC-PapersOnline

Citation (APA)
Du, Z., Negenborn, R. R., & Reppa, V. (2021). Multi-vessel cooperative speed regulation for ship manipulation in towing scenarios. *IFAC-PapersOnline*, *54*(16), 384-389. https://doi.org/10.1016/j.ifacol.2021.10.120

Available online at www.sciencedirect.com

ScienceDirect

IFAC PapersOnLine 54-16 (2021) 384–389

Multi-Vessel Cooperative Speed Regulation for Ship Manipulation in Towing Scenarios

Zhe Du, Rudy R. Negenborn, Vasso Reppa

Department of Maritime and Transport Technology, Delft University of Technology, Delft, The Netherlands (e-mail: Z.Du@tudelft.nl).

Abstract: This paper proposes a multi-agent control scheme for multiple physically interconnected tugboats performing a ship towing process. These tugs are coordinated by two control layers. In the higher layer, the supervisory controller outputs the desired towing forces and reference trajectories for the tugs. This information is used by a tug's local controller in the lower layer to calculate the thruster forces and moment for manipulating the ship. The control strategy is based on the model predictive control concept, with the performance function designed by using the position and velocity error to make the ship follow waypoints and speed profile. A distributed control architecture is designed based on the alternating direction method of multipliers (ADMM) to reach a consensus between the predicted position generated by the tug controllers and the reference trajectory generated by the supervisory controller. Simulation experiments illustrate that the proposed method ensures the smooth and efficient maneuverability of the towing process.

Keywords: Cooperative control, Autonomous surface vessels, Multi-vessel systems, Physical-connected systems, Speed regulation, Distributed MPC

1. INTRODUCTION

Autonomous Surface Vessels (ASVs) have been applied for carrying out various types of missions (Liu et al. (2016)). In recent years, the high mission complexity motivates the research of the multi-vessel systems. There are two types of connections for this kind of system: cyber-connected and physical-connected. In the first case, all vessels are clustered within a safe distance forming a certain formation shape (Chen et al. (2018)), and the connection is realized through a digital network. In the second case, there is a physical link (through a cable (Arrichiello et al. (2011)) or direct attachment (Bidikli et al. (2016))) between vessels. Physical connection often involves a floating object, manipulated by multiple vessels to the desired states. Compared to the cyber-connected system, this type has less ability of maneuvering.

As a typical application of the physical-connected multi-vessel systems, the ship-towing manipulation is an important but also hazardous and challenging task in the shipping industry. In previous research, we have investigated a set of cooperative control schemes for a ship-towing system to deal with the position and heading control of the ship (Du et al. (2020)), the robust control against environmental disturbances (Du et al. (2021a)), and the distance control for collision avoidance (Du et al. (2021b)). All these works focus on implementing the mission of ship manipulation but pay less attention to the towing process. Since the vessel speed is relevant to the smoothness of the motion, the efficiency of the navigation and the fuel consumption, especially in the restricted inland waterways (Tarelko and Rudzki (2020)), it is necessary to take into consideration the speed regulation for such a maneuverability-restricted system. In practice, before carrying out the towage operations speed recommendations (Shipowner (The Shipowners' Club (2015)) and DNV classification society (Hansen (2014))) are given for dealing with different situations, such as bad weather and variable water depth conditions.

The vessel speed regulation is meant for improving the reliability of small high-speed vessels (Sorensen et al. (2017)). Scholars in (Klinger et al. (2017)) design an adaptive yaw and speed controller using the backstepping method for tracking the desired surge speed and heading angle. In (Lv et al. (2019)), authors combine the backstepping-based surge speed controller and the hamiltonian system-based energy controller for speed and heading control of unmanned surface vehicles. In (Peng et al. (2021)), researchers combine an adaptive identification and a PWM-driven model predictive controller to deal with the surge speed control problem under the unknown model parameters of surge and propeller dynamics.

The above research works consider a single vessel case. For the physical-connected multi-vessel system that we consider, there is a lack of research focusing on speed regulation. Thus, the goal and the main contribution of this work is to propose a multi-agent cooperative speed regulation scheme for a physically interconnected multi-ASV system performing a towing process. The multi-agent control architecture facilitates the scalability of the ship towing process (Negenborn and Maestre (2013)), where the number of tugboats depends on the weather conditions and the length of the ship (Hensen (2003)). The proposed control scheme can make the multiple autonomous tugs cooperatively manipulate a ship to the desired position with the desired heading and follow the recommended speed profiles.

10.1016/j.ifacol.2021.10.120

The remainder of this paper is organized as follows: Section 2 formulates the problem of the ship towing. The proposed cooperative control approach is given in Section 3. In Section 4, simulation experiments are carried out to assess the proposed method. Conclusions and future research plans are given in Section 5.

2. PROBLEM STATEMENT

The objective of this work is to design a cooperative control scheme to manipulate a ship smoothly and efficiently to the desired states by two autonomous tugs. The motion of each individual vessel is represented by the 3-DoF (degree of freedom) hydrodynamic model (Fossen (2011)):

$$\begin{aligned}\dot{\boldsymbol{\eta}}_*(t) &= \boldsymbol{R}\big(\psi_*(t)\big)\boldsymbol{\nu}_*(t)\\ \boldsymbol{M}_*\dot{\boldsymbol{\nu}}_*(t)+\boldsymbol{C}_*\big(\boldsymbol{\nu}_*(t)\big)\boldsymbol{\nu}_*(t)+\boldsymbol{D}_*\boldsymbol{\nu}_*(t) &= \boldsymbol{\tau}_*(t),\end{aligned} \tag{1}$$

where $*$ stands for S (ship) or i (tug, $i = 1,\ 2$); $\boldsymbol{\eta}_*(t) = [x_*(t)\ y_*(t)\ \psi_*(t)]^{\mathrm{T}} \in \mathbb{R}^3$ is the position vector in the world frame including position coordinates $\big(x_*(t),\ y_*(t)\big)$ and heading $\psi_*(t)$; $\boldsymbol{\nu}_*(t) = [u_*(t)\ v_*(t)\ r_*(t)]^{\mathrm{T}} \in \mathbb{R}^3$ is the velocity vector in the Body-fixed frame containing the velocity of surge $u_*(t)$, sway $v_*(t)$ and yaw $r_*(t)$; $\boldsymbol{R} \in \mathbb{R}^{3\times3}$ is the rotation matrix from the body frame to the world frame, which is a function of heading; $\boldsymbol{M}_* \in \mathbb{R}^{3\times3}$, $\boldsymbol{C}_* \in \mathbb{R}^{3\times3}$ and $\boldsymbol{D}_* \in \mathbb{R}^{3\times3}$ are the mass (inertia), Coriolis-Centripetal and damping matrix, respectively; $\boldsymbol{\tau}_*(t) = [\tau_{*\mathrm{u}}(t)\ \tau_{*\mathrm{v}}(t)\ \tau_{*\mathrm{r}}(t)]^{\mathrm{T}} \in \mathbb{R}^3$ is the controllable input referring to the forces $\tau_{*\mathrm{u}}(t)$, $\tau_{*\mathrm{v}}(t)$ and moment $\tau_{*\mathrm{r}}(t)$ in the Body-fixed frame. The motion of a vessel in this model can be decomposed into speed (surge) and steering (sway and yaw) parts. Speed regulation in this paper refers to regulating the magnitude of the surge velocity.

The controllable inputs of the ship ($\boldsymbol{\tau}_S(t)$) are the forces from the towing lines applied by the two tugs (see (Du et al. (2020)) for details on modelling of the ship towing system), which can be expressed as:

$$\begin{aligned}\boldsymbol{\tau}_S(t) &= \boldsymbol{\tau}_{S_1}(t)+\boldsymbol{\tau}_{S_2}(t) = \sum_{i=1}^{2}\boldsymbol{B}_S\big(\alpha_i(t)\big)F_i(t)\\ \boldsymbol{B}_S &= \begin{bmatrix}\cos\big(\alpha_i(t)\big)\\ \sin\big(\alpha_i(t)\big)\\ l_i\sin\big(\alpha_i(t)\big)\end{bmatrix} \quad (i=1,2),\end{aligned} \tag{2}$$

where $F_i(t)$ is the towing force; $\boldsymbol{B}_S$ is the configuration matrix which is a function of the towing angle ($\alpha_i(t)$); l_i is the distance from the center of gravity of the ship to the ship stern (l_1) or the ship bow (l_2).

To increase the flexibility of the towing process, the actuator system of a tug usually contains two stern azimuth thrusters and one bow tunnel thruster, known as the *ASD tug*, that can create omnidirectional forces and moments (Hensen (2003)). The inputs of the i-th tug ($\boldsymbol{\tau}_i(t)$) are expressed as:

$$\begin{aligned}\boldsymbol{\tau}_i(t) &= \boldsymbol{B}_i\big(\beta_i(t)\big)F_i^{'}(t)+\boldsymbol{\tau}_{T_i}(t)\\ \boldsymbol{B}_i &= \begin{bmatrix}\cos\big(\beta_i(t)\big)\\ \sin\big(\beta_i(t)\big)\\ l_{\mathrm{T}_i}\sin\big(\beta_i(t)\big)\end{bmatrix} \quad (i=1,2),\end{aligned} \tag{3}$$

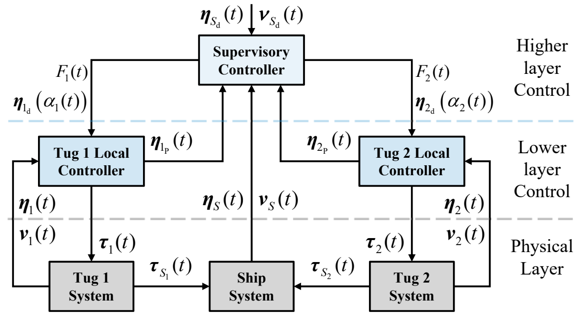

Fig. 1. Multi-vessel system control diagram.

where $\boldsymbol{B}_i$ is the configuration matrix of the tugs; $\beta_i(t)$ is the tug angle; l_{T_i} is the distance from the center of gravity of the tug to the tug stern (l_{T_2}) or the tug bow (l_{T_1}); $F_i^{'}(t)$ is the force applied through a controlled winch onboard the tugboat to the towline. Assuming no force loss on the towline, then $F_i^{'}(t) \equiv F_i(t)$. The term $\boldsymbol{\tau}_{T_i}(t)\in\mathbb{R}^3$ are the forces and moment to move the tug.

3. DISTRIBUTED COOPERATIVE SPEED REGULATION SCHEME

The cooperative control scheme is based on the distributed multi-layer control structure as shown in Fig. 1. At the higher layer, according to the ship reference path $\boldsymbol{\eta}_{S_\mathrm{d}}(t)$, speed profile $\boldsymbol{\nu}_{S_\mathrm{d}}(t)$ and current states $\boldsymbol{\eta}_S(t)$, $\boldsymbol{\nu}_S(t)$, the supervisory controller (located on the ship) calculates the towing forces $F_i(t)$ and the reference trajectory of the tugs $\boldsymbol{\eta}_{i_\mathrm{d}}\big(\alpha_i(t)\big)$, which is a function of the towing angles $\alpha_i(t)$. At the lower layer, the tug local controller uses the calculated above data and the current states of tugs $\boldsymbol{\eta}_i(t)$, $\boldsymbol{\nu}_i(t)$ to first calculate the predicted position $\boldsymbol{\eta}_{i_\mathrm{P}}(t)$, and share this information with the supervisory controller to reach a consensus between the predicted position and the tug reference trajectory ($\boldsymbol{\eta}_{i_\mathrm{P}}(t) = \boldsymbol{\eta}_{i_\mathrm{d}}(t)$). Then, the supervisory controller updates the towing forces and angles. When the consensus is achieved, the tug local controller outputs the thruster forces and moment $\boldsymbol{\tau}_i(t)$ to the tug system. Finally, the two autonomous tugs provide forces and moment ($\boldsymbol{\tau}_{S_1}(t)$ and $\boldsymbol{\tau}_{S_2}(t)$) through a winch onboard to manipulate the ship.

3.1 Control Performance Function Design

The manipulated ship in such a maneuverability-restricted towing system requires more time to respond to the control order provided by tugboats, making necessary to take actions in advance over the prediction horizon. There are also multiple control constraints such as kinematics, kinetics, and actuator saturation. Considering the above features, the Model Predictive Control (MPC) is applied for the design of the controllers.

For the Supervisory Controller, the objective is to make the ship follow the waypoints and speed profile. The performance function of the ship at sampled time k is designed as:

$$\begin{aligned}J_S(k) &= \boldsymbol{e}_{\eta_S}^{\mathrm{T}}(k)\boldsymbol{W}_{S1}\boldsymbol{e}_{\eta_S}(k)+\boldsymbol{e}_{\nu_S}^{\mathrm{T}}(k)\boldsymbol{W}_{S2}\boldsymbol{e}_{\nu_S}(k)\\ \boldsymbol{e}_{\eta_S}(k) &= \boldsymbol{\eta}_{S_\mathrm{P}}(k)-\boldsymbol{\eta}_{S_\mathrm{d}}(k)\\ \boldsymbol{e}_{\nu_S}(k) &= \boldsymbol{\nu}_{S_\mathrm{P}}(k)-\boldsymbol{\nu}_{S_\mathrm{d}}(k),\end{aligned} \tag{4}$$

where $\boldsymbol{e}_{\eta_S}(k)\in\mathbb{R}^3$ and $\boldsymbol{e}_{\nu_S}(k)\in\mathbb{R}^3$ are the position and velocity error of the ship; $\boldsymbol{\eta}_{S_{\mathrm{P}}}(k)\in\mathbb{R}^3$ and $\boldsymbol{\nu}_{S_{\mathrm{P}}}(k)\in\mathbb{R}^3$ are the predicted position and velocity of the ship; $\boldsymbol{\eta}_{S_{\mathrm{d}}}(k)\in\mathbb{R}^3$ and $\boldsymbol{\nu}_{S_{\mathrm{d}}}(k)\in\mathbb{R}^3$ are the desired position and velocity of the ship, where $\boldsymbol{\eta}_{S_{\mathrm{d}}}(k)$ is the data of next waypoint, and $\boldsymbol{\nu}_{S_{\mathrm{d}}}(k)$ is the speed profile; $\boldsymbol{W}_{S1} = diag(w_{Sx}\ w_{Sy}\ w_{S\psi})$ and $\boldsymbol{W}_{S2} = diag(w_{Su}\ w_{Sv}\ w_{Sr})$ are the weight coefficients.

For each waypoint-following task, the value of position error at the beginning is maximum, the controller focuses on approaching the waypoint and increases the ship's speed. As the value of position error reduces, the velocity part is gradually dominant in the performance function, the speed profile-following task then starts to perform. Thus, it is necessary to add a weight factor in the position part to normalize the order of magnitude between the position and velocity errors, and to reduce the sensitivity of the controller to the waypoint distance. The weight factor is designed as a diagonal matrix:

$$\boldsymbol{P}(t) = \begin{bmatrix} 1/d_{Wj}(t) & & \\ & 1/d_{Wj}(t) & \\ & & 1 \end{bmatrix}, \tag{5}$$

$$d_{\mathrm{W}j}(t) = \sqrt{\left(x_S(t) - x_{\mathrm{W}j}\right)^2 + \left(y_S(t) - y_{\mathrm{W}j}\right)^2}, \tag{6}$$

where $d_{\mathrm{W}j}(t)$ is the distance from current position of the ship $(x_S(t), y_S(t))$ to the waypoint j $(x_{\mathrm{W}j}, y_{\mathrm{W}j})$. By applying (5) and (6), the performance function in (4) is revised as:

$$J_S(k) = \boldsymbol{e}_{\eta_S}^{\mathrm{T}}(k)\boldsymbol{W}_{S1}\boldsymbol{P}(k)\boldsymbol{e}_{\eta_S}(k) + \boldsymbol{e}_{\nu_S}^{\mathrm{T}}(k)\boldsymbol{W}_{S2}\boldsymbol{e}_{\nu_S}(k). \tag{7}$$

For the Tug Local Controller, the objective is to track the tug reference trajectory. The performance function of the tug i at sample time k is designed as:

$$\begin{aligned} &J_i(k) = \boldsymbol{e}_{\eta_i}^{\mathrm{T}}(k)\boldsymbol{W}_{i1}\boldsymbol{e}_{\eta_i}(k) + \boldsymbol{\nu}_{i\mathrm{P}}^{\mathrm{T}}(k)\boldsymbol{W}_{i2}\boldsymbol{\nu}_{i\mathrm{P}}(k) \\ &\boldsymbol{e}_{\eta_i}(k) = \boldsymbol{\eta}_{i\mathrm{P}}(k) - \boldsymbol{\eta}_{i_{\mathrm{d}}}(k), \end{aligned} \tag{8}$$

where $\boldsymbol{e}_{\eta_i}(k)\in\mathbb{R}^3$ is the position error of the tug i; $\boldsymbol{\eta}_{i\mathrm{P}}(k)\in\mathbb{R}^3$ and $\boldsymbol{\nu}_{i\mathrm{P}}(k)\in\mathbb{R}^3$ are the predicted position and velocity of the tug i; $\boldsymbol{\eta}_{i_{\mathrm{d}}}(k)$ is the tug reference trajectory; $\boldsymbol{W}_{i1} = diag(w_{ix}\ w_{iy}\ w_{i\psi})$ and $\boldsymbol{W}_{i2} = diag(w_{iu}\ w_{iv}\ w_{ir})$ are the weight coefficients.

3.2 MPC-based Control Strategy

Based on the above performance function, the MPC strategy for the supervisory and tug local controllers are formulated as:

$$U_S = \min_{\boldsymbol{\tau}_S} \sum_{h=1}^{H_{\mathrm{P}}} J_S(k+h|\,k), \tag{9}$$

$$U_i = \min_{\boldsymbol{\tau}_{T_i}} \sum_{h=1}^{H_{\mathrm{P}}} J_i(k+h|\,k), \tag{10}$$

subject to the *dynamics* and *operational* constraints,

where U_S and U_i are the control inputs of the ship and tug i; H_{P} is the length of the prediction horizon; h is the hth time prediction step; $J_S(k+h|\,k)$ and $J_i(k+h|\,k)$ are the prediction made at k about the cost of the ship and tug i at $k+h$, respectively. The constraints are defined below.

The dynamics of the ship and the tug i in (4) and (8), are calculated by discretizing the dynamic model in Section 2 with a sample time T_s:

$$\begin{aligned} &\boldsymbol{\eta}_{S_{\mathrm{P}}}(k+1) = \boldsymbol{\eta}_{S_{\mathrm{P}}}(k) + \textstyle\int_{kT_s}^{(k+1)T_s} \boldsymbol{R}(\psi_S(t))\boldsymbol{\nu}_S(t)dt \\ &\boldsymbol{\nu}_{S_{\mathrm{P}}}(k+1) = \boldsymbol{\nu}_{S_{\mathrm{P}}}(k) + \textstyle\int_{kT_s}^{(k+1)T_s} \boldsymbol{M}_S^{-1}[-\boldsymbol{C}_S(\boldsymbol{\nu}_S(t))\boldsymbol{\nu}_S(t) \\ &-\boldsymbol{D}_S\boldsymbol{\nu}_S(t) - \boldsymbol{B}(\alpha_1(t))F_1(t) + \boldsymbol{B}(\alpha_2(t))F_2(t)]dt, \end{aligned} \tag{11}$$

$$\begin{aligned} &\boldsymbol{\eta}_{i\mathrm{P}}(k+1) = \boldsymbol{\eta}_{i\mathrm{P}}(k) + \textstyle\int_{kT_s}^{(k+1)T_s} \boldsymbol{R}(\psi_i(t))\boldsymbol{\nu}_i(t)dt \\ &\boldsymbol{\nu}_{i\mathrm{P}}(k+1) = \boldsymbol{\nu}_{i\mathrm{P}}(k) + \textstyle\int_{kT_s}^{(k+1)T_s} \boldsymbol{M}_i^{-1}[-\boldsymbol{C}_i(\boldsymbol{\nu}_i(t))\boldsymbol{\nu}_i(t) \\ &-\boldsymbol{D}_i\boldsymbol{\nu}_i(t) + \boldsymbol{B}_i(\beta_i(t))F_i(t) + \boldsymbol{\tau}_{T_i}(t)]dt. \end{aligned} \tag{12}$$

For all k and $i = 1, 2$, the operational constraints for the control inputs are expressed as:

$$-30^\circ \le \alpha_i(k) < 30^\circ \tag{13}$$

$$0 \le F_i(k) \le F_{i\,\max} \tag{14}$$

$$-\boldsymbol{\tau}_{i\,\max} \le \boldsymbol{\tau}_i(k) \le \boldsymbol{\tau}_{i\,\max} \tag{15}$$

$$|\dot{\alpha}_i(k)| \le \bar{\alpha}_i \tag{16}$$

$$\left|\dot{F}_i(k)\right| \le \bar{F}_i \tag{17}$$

where $F_{i\,\max}$ is the maximum value of towing force that the two towing lines withstand; $\boldsymbol{\tau}_{i\,\max}$ is the maximum value of the thruster forces and moment; $\bar{\alpha}_i$ and $\bar{F}_i$ are the maximum change rate value of towing angle and force, respectively.

Constraints (13), (14) and (15) model the saturation of the towing forces, towing angles and thruster forces, stemming from the physical laws and maritime practice (Hensen (2003)); (16) and (17) limit the change rate of the towing angles and forces, in order to make the tug reference trajectory smooth improving the performance of the trajectory tracking.

3.3 ADMM-based Distributed Control Scheme

The Altering Direction Method of Multipliers (ADMM) is a widely used algorithm well suited to distributed optimization, whose idea is to blend the dual ascent optimization approach with the augmented Lagrangians method of multipliers, which obtains superior decomposability and convergence properties (Stephen et al. (2010)).

In our case, the supervisory controller provides the reference trajectory to the two tug local controllers $(\boldsymbol{\eta}_{i_{\mathrm{d}}}(k))$, which is calculated by the desired geometrical relationship between the ship and tugs (shown in Fig. 2) (Du et al. (2020)); i.e. for $i = 1, 2$:

$$\begin{aligned} \boldsymbol{\eta}_{i\mathrm{d}}(k) = \boldsymbol{\eta}_{S_{\mathrm{P}}}(k) + (l_{\mathrm{tow}_i} + l_{\mathrm{T_i}})\boldsymbol{E}_i(\psi_{S_{\mathrm{P}}}(k), \alpha_i(k)) + \\ l_i\boldsymbol{F}_i(\psi_{S_{\mathrm{P}}}(k)) + \alpha_i(k)[0\ 0\ 1]^{\mathrm{T}}, \end{aligned} \tag{18}$$

where l_{tow_i} is the length of the towing line; $\boldsymbol{E}_i\in\mathbb{R}^3$ and $\boldsymbol{F}_i\in\mathbb{R}^3$ are the vectors related to the predicted heading of the ship and the towing angles, formulated as:

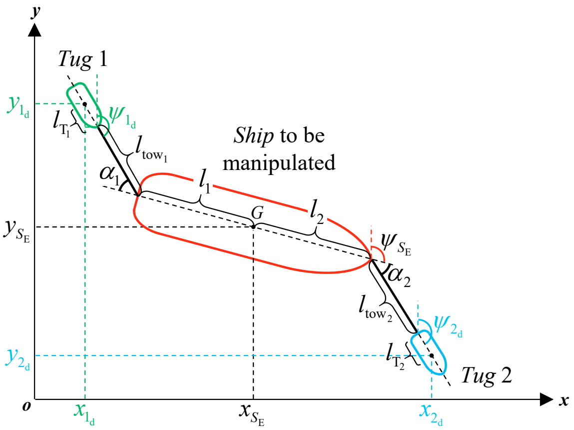

Fig. 2. Kinematic model of the ship towing system.

$$\boldsymbol{E}_i = (-1)^i \begin{bmatrix} \sin(\psi_{S_\mathrm{P}}(k) + \alpha_i(k)) \\ \cos(\psi_{S_\mathrm{P}}(k) + \alpha_i(k)) \\ 0 \end{bmatrix}, \tag{19}$$

$$\boldsymbol{F}_i = (-1)^i \begin{bmatrix} \sin(\psi_{S_\mathrm{P}}(k)) \\ \cos(\psi_{S_\mathrm{P}}(k)) \\ 0 \end{bmatrix}. \tag{20}$$

Thus, the consensus between the ship and tugs can be achieved by making the tug's predicted position equal to the tug reference trajectory. The augmented Lagrangian form at time instant k can be formulated as:

$$L_p\big(\boldsymbol{\tau_S}(k), \boldsymbol{\tau}_{T_i}(k), \lambda_i(k)\big) = J_S\big(\boldsymbol{\tau}_S(k)\big) + \sum_{i=1}^{2} \Big(J_i\big(\boldsymbol{\tau}_{T_i}(k)\big) \\ + \lambda_i^\mathrm{T}(k)[\boldsymbol{\eta}_{i\mathrm{P}}(k) - \boldsymbol{\eta}_{i_\mathrm{d}}(k)] + (\rho/2)\left\|\boldsymbol{\eta}_{i\mathrm{P}}(k) - \boldsymbol{\eta}_{i_\mathrm{d}}(k)\right\|_2^2 \Big), \tag{21}$$

where $\lambda_i(k)$ is the Lagrange multiplier or dual variable, and ρ is the penalty parameter. According to (18)-(20), $\boldsymbol{\eta}_{i_\mathrm{d}}(k)$ is a function of the towing angle $\alpha_i(k)$ and ship's heading $\psi_{S_\mathrm{P}}(k)$. The variable $\alpha_i(k)$ is an element of the $\boldsymbol{\tau}_S(k)$, and $\psi_{S_\mathrm{P}}(k)$ can be calculated by the ship dynamics (11). Thus, $\boldsymbol{\eta}_{i_\mathrm{d}}(k)$ is a function of $\boldsymbol{\tau}_S(k)$:

$$\boldsymbol{\eta}_{i_\mathrm{d}}(k) = f_i\big(\boldsymbol{\tau}_S(k)\big). \tag{22}$$

Similarly, $\boldsymbol{\eta}_{i\mathrm{P}}(k)$ can be calculated based on the tug dynamics (12), as a function of $\boldsymbol{\tau}_{T_i}(k)$:

$$\boldsymbol{\eta}_{i\mathrm{P}}(k) = g_i\big(\boldsymbol{\tau}_{T_i}(k)\big). \tag{23}$$

According to (21) - (23), the ADMM form of the iterations are formulated as:

$$\boldsymbol{\tau}_{T_i}^s(k) := \operatorname*{arg\,min}_{\boldsymbol{\tau}_{T_i}(k)} \bigg(J_i\big(\boldsymbol{\tau}_{T_i}(k)\big) + \lambda_i^{s-1}(k)^\mathrm{T} \Big[g_i\big(\boldsymbol{\tau}_{T_i}(k)\big) - \\ f_i\big(\boldsymbol{\tau}_S^{s-1}(k)\big)\Big] + (\rho/2) \Big\| g_i\big(\boldsymbol{\tau}_{T_i}(k)\big) - f_i\big(\boldsymbol{\tau}_S^{s-1}(k)\big)\Big\|_2^2 \bigg), \tag{24}$$

$$\boldsymbol{\tau}_S^s(k) := \operatorname*{arg\,min}_{\boldsymbol{\tau}_S(k)} \bigg(J_S\big(\boldsymbol{\tau}_S(k)\big) + \sum_{i=1}^{2} \Big(-\lambda_i^{s-1}(k)^\mathrm{T} f_i\big(\boldsymbol{\tau}_S(k)\big) \\ + (\rho/2) \Big\| g_i\big(\boldsymbol{\tau}_{T_i}^s(k)\big) - f_i\big(\boldsymbol{\tau}_S(k)\big)\Big\|_2^2 \Big) \bigg), \tag{25}$$

$$\lambda_i^s(k) := \lambda_i^{s-1}(k) + \rho_i \Big(g_i\big(\boldsymbol{\tau}_{T_i}^s(k)\big) - f_i\big(\boldsymbol{\tau}_S^s(k)\big)\Big), \tag{26}$$

where s is the iteration, $\cdot^s$ stands for the corresponding variable at the sth iteration.

The termination criterion for the iterations is provided according to the following conditions:

$$\left\|\boldsymbol{R}_{\mathrm{pri},i}^s(k)\right\|_2 = \Big\| g_i\big(\boldsymbol{\tau}_{T_i}^s(k)\big) - f_i\big(\boldsymbol{\tau}_S^s(k)\big)\Big\|_2 \le \varepsilon_{\mathrm{pri},i}^s(k) \\ \left\|\boldsymbol{R}_{\mathrm{dual},i}^s(k)\right\|_2 = \Big\| f_i\big(\boldsymbol{\tau}_S^s(k)\big) - f_i\big(\boldsymbol{\tau}_S^{s-1}(k)\big)\Big\|_2 \le \varepsilon_{\mathrm{dual},i}^s(k), \tag{27}$$

where $\boldsymbol{R}_{\mathrm{pri},i}^s$ and $\boldsymbol{R}_{\mathrm{dual},i}^s$ are the primal and dual residual at iteration s; $\varepsilon_{\mathrm{pri},i}^s > 0$ and $\varepsilon_{\mathrm{dual},i}^s > 0$ are feasibility tolerances.

4. SIMULATION EXPERIMENT

A simulation experiment was carried out to show the application of the proposed method to a ship-towing system of small-scale vessels and the comparison with a non-speed regulation method.

The model of the two tugs are represented by the "*TitoNeri*" developed by TU Delft (Skjetne et al. (2004)), while the ship is represented by the "*CyberShip II*" (Haseltalab and Negenborn (2019)). The parameters of the vessel model and the towing system can be found in (Du et al. (2020)).

The value of weight coefficients are set as: $\boldsymbol{W}_{S1} = diag(1 \;\; 1 \;\; 0.2)$, $\boldsymbol{W}_{S2} = diag(200 \;\; 20 \;\; 20)$; $\boldsymbol{W}_{i1} = diag(1 \;\; 1 \;\; 1)$, $\boldsymbol{W}_{i2} = diag(2 \;\; 2 \;\; 2)$. The parameters of operational constraints are set as: $F_{i\,\max} = 3$ N, $\boldsymbol{\tau}_{i\,\max} = 10$ N, $\bar{\alpha}_i = 5°/\mathrm{s}$, $\bar{F}_i = 0.1$ N/s. The prediction horizon H_P is set to 3. The objective is to manipulate the ship from initial states $\boldsymbol{\eta}_{S_0} = [0 \;\; 0 \;\; 78.7]^\mathrm{T}$ to the target states $\boldsymbol{\eta}_{S_t} = [20 \;\; -20 \;\; 0]^\mathrm{T}$. Between the origin ($\mathrm{W_{pO}}$) and the destination ($\mathrm{W_{pD}}$), there are three waypoints, whose coordinates are: $\mathrm{W_{p1}} = (7.5, 1.5)$, $\mathrm{W_{p2}} = (15, 3)$, $\mathrm{W_{p3}} = (20, 10)$.

We consider two scenarios, A and B. In the scenario A, the position weight w_{Sx} and w_{Sy} are constant and there is no speed profile, the second part in the cost function (4) is the velocity as in (8). In the control scenario B, the position weight w_{Sx} and w_{Sy} are time-varying calculated by (5) and (6). The speed profile is set as: from $\mathrm{W_{pO}}$ to $\mathrm{W_{p2}}$, $\boldsymbol{\nu}_{S_{\mathrm{d}1}} = [0.15 \;\; 0 \;\; 0]^\mathrm{T}$; from $\mathrm{W_{p2}}$ to $\mathrm{W_{pD}}$, $\boldsymbol{\nu}_{S_{\mathrm{d}2}} = [0.10 \;\; 0 \;\; 0]^\mathrm{T}$; at $\mathrm{W_{pD}}$, $\boldsymbol{\nu}_{S_{\mathrm{d}3}} = [0 \;\; 0 \;\; 0]^\mathrm{T}$.

The towing process is shown in Fig. 3. For the first two waypoint-following, the three vessels in the two scenarios have similar trajectories where the three trajectories overlap in the straight path. However, for the next steering process, the performance is much different. It is observed that the three trajectories in scenario A have much more fluctuations than those in scenario B, especially for the two tugs. From the view of the time cost, comparing the time for arriving at each waypoint, scenario B is more efficient than scenario A. Thus, although the two scenarios achieve to manipulate the ship to the desired states, the vessels in scenario B have smoother trajectories and faster accomplishment. The reason can be analyzed by looking into the vessel's states.

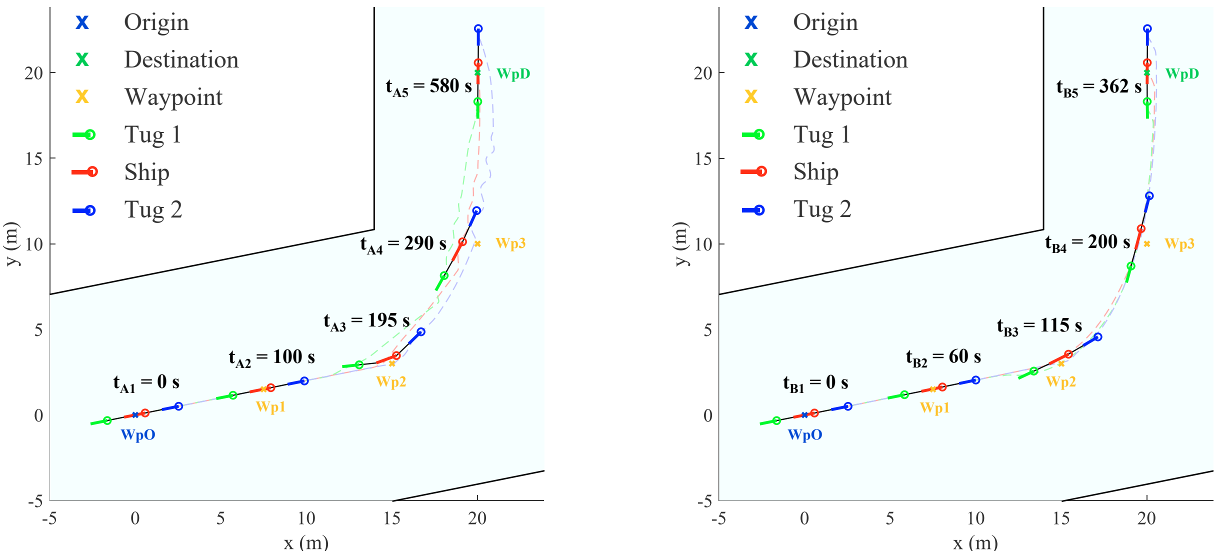

(a) (b)

Fig. 3. Towing process: (a) Simulation in scenario A; (b) Simulation in scenario B.

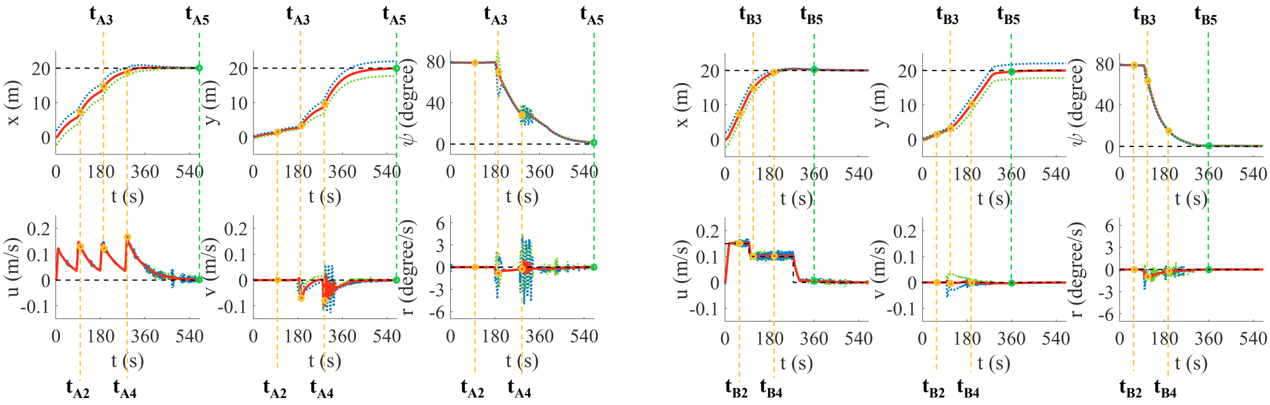

(a) (b)

Fig. 4. Six states of the ship (red bold line) and the two tugs (green dotted line for Tug 1 and blue dotted line for Tug 2), the black dashed line stands for their desired value, the circles are the sampled time in Fig. 3: (a) Simulation in scenario A; (b) Simulation in scenario B.

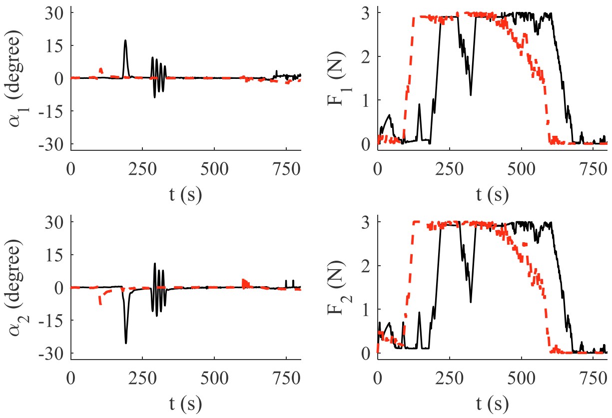

Fig. 5. Towing angles and forces: the black solid line is scenario A, the red dashed line is scenario B.

The time-varying states of the ship and two tugs are shown in Fig. 4. The main difference between the two scenarios is the changes in velocity. In scenario B, the ship's surge speed stably follows its profile from 0.15 m/s decreasing to 0.1 m/s and finally fixing at 0 m/s, the ship's sway and yaw speed vary around zero. The only one-time change of the yaw speed is when the towing system starts to conduct steering operation (around 100 s). However, the ship's velocity in scenario A has much more oscillations. For the surge speed, there are four "jagged" changes in the towing process. These "jags" are derived from the changes of the position errors in each time of the waypoint following (totally four times), which is from the maximum value at the beginning decreasing to the minimum value in the end. With a constant position weight, such changes motivate the surge speed to vary from the highest to the lowest. Similarly for the ship's sway and yaw speed, because of the steering operation of following the third waypoint and the destination point, the sway and yaw speed jump to a high value at the beginning, while the two tugs have to carry out more frequent and larger changes in sway and yaw motion to satisfy the high sway and yaw velocities of the ship. Thus, there are such frequent fluctuations for the three trajectories in scenario A.

Fig. 5 shows the time-varying towing angles and forces, and all the variables satisfy the operational constraints. For the towing angles, the values in scenario B are obviously smaller than those in scenario A. For the towing forces, the change rates and settling time in scenario B are noticed lower and less than those in scenario A, respectively. Thus, the proposed control scheme has better motion smoothness and time efficiency.

5. CONCLUSIONS AND FUTURE RESEARCH

This paper focuses on the speed regulation of a physically connected multi-vessel system for performing a ship-towing process. We propose a distributed cooperative multi-layer control scheme to make the multiple autonomous tugs cooperatively not only move the ship to the destination with the desired heading but also make it following the waypoints and recommended speed profiles. The distributed control structure is built based on the ADMM strategy to reach the consensus between the ship and the tugs. In the higher layer, the supervisory controller outputs the desired towing forces and reference trajectory for the tugs. In the lower layer, the tug local controller uses the above data to calculate the thruster forces and moment for manipulating the ship. The control strategy in the controllers is based on the MPC method, whose cost function consists of position and velocity errors. A time-varying weight factor is designed for normalizing the two errors to make the ship follow both the waypoints and the speed profile.

Simulation experiments indicate that the proposed method has a better performance in the smoothness of the system motion and the efficiency of the towing process. Future research will focus on making the control scheme robust against disturbances and performing collision avoidance.

ACKNOWLEDGEMENTS

This research is supported by the China Scholarship Council under Grant 201806950080, the Researchlab Autonomous Shipping (RAS) of Delft University of Technology, and the INTERREG North Sea Region Grant "AVATAR" funded by the European Regional Development Fund.

REFERENCES

Arrichiello, F., Heidarsson, H.K., Chiaverini, S., and Sukhatme, G.S. (2011). Cooperative caging and transport using autonomous aquatic surface vehicles. *Intelligent Service Robotics*, 5(1), 73–87.

Bidikli, B., Tatlicioglu, E., and Zergeroglu, E. (2016). Robust dynamic positioning of surface vessels via multiple unidirectional tugboats. *Ocean Engineering*, 113, 237–245.

Chen, L., Hopman, H., and Negenborn, R.R. (2018). Distributed model predictive control for vessel train formations of cooperative multi-vessel systems. *Transportation Research Part C: Emerging Technologies*, 92, 101–118.

Du, Z., Negenborn, R.R., and Reppa, V. (2021a). Cooperative multi-agent control for autonomous ship towing under environmental disturbances. *IEEE/CAA Journal of Automatica Sinica*, 8(8), 1365–1379.

Du, Z., Reppa, V., and Negenborn, R.R. (2020). Cooperative control of autonomous tugs for ship towing. In *Proceedings of the 21st IFAC World Congress*, 14671–14676. Berlin, Germany.

Du, Z., Reppa, V., and Negenborn, R.R. (2021b). Mpc-based colregs compliant collision avoidance for a multi-vessel ship-towing system. In *Proceedings of the European Control Conference, ECC'21*. Rotterdam, the Netherlands.

Fossen, T.I. (2011). *Handbook of Marine Craft Hydrodynamics and Motion Control*. John Wiley & Sons, Chichester, West Sussex, UK.

Hansen, R.H. (2014). DNV Towing Recommendations. techreport, Det Norske Veritas.

Haseltalab, A. and Negenborn, R.R. (2019). Model predictive maneuvering control and energy management for all-electric autonomous ships. *Applied Energy*, 251(113308), 1–27.

Hensen, H. (2003). *Tug Use in Port: A Practical Guide*. Nautical Institute, London, UK.

Klinger, W.B., Bertaska, I.R., von Ellenrieder, K.D., and Dhanak, M.R. (2017). Control of an unmanned surface vehicle with uncertain displacement and drag. *IEEE Journal of Oceanic Engineering*, 42(2), 458–476.

Liu, Z., Zhang, Y., Yu, X., and Yuan, C. (2016). Unmanned surface vehicles: An overview of developments and challenges. *Annual Reviews in Control*, 41, 71–93.

Lv, C., Yu, H., Chi, J., Xu, T., Zang, H., lue Jiang, H., and Zhang, Z. (2019). A hybrid coordination controller for speed and heading control of underactuated unmanned surface vehicles system. *Ocean Engineering*, 176, 222–230.

Negenborn, R.R. and Maestre, J.M. (2013). *On 35 Approaches for Distributed MPC Made Easy*, 1–37. Intelligent Systems, Control and Automation: Science and Engineering. Springer Netherlands.

Peng, Z., Meng, C., Liu, L., Wang, D., and Li, T. (2021). PWM-driven model predictive speed control for an unmanned surface vehicle with unknown propeller dynamics based on parameter identification and neural prediction. *Neurocomputing*, 432, 1–9.

Skjetne, R., Smogeli, Ø., and Fossen, T.I. (2004). Modeling, identification, and adaptive maneuvering of Cybership II: A complete design with experiments. *IFAC Proceedings Volumes*, 37(10), 203–208.

Sorensen, M.E.N., Breivik, M., and Eriksen, B.O.H. (2017). A ship heading and speed control concept inherently satisfying actuator constraints. In *Proceedings of the 2017 IEEE Conference on Control Technology and Applications*, 323–330. Mauna Lani, HI.

Stephen, B., Neal, P., Eric, C., Borja, P., and Jonathan, E. (2010). Distributed optimization and statistical learning via the alternating direction method of multipliers. *Foundations and Trends in Machine Learning*, 3(1), 1–122.

Tarelko, W. and Rudzki, K. (2020). Applying artificial neural networks for modelling ship speed and fuel consumption. *Neural Computing and Applications*, 32(23), 17379–17395.

The Shipowners' Club (2015). Tugs and Tows – A practical safety and operational guide. London, UK.